https://doi.org/10.63181/ujcvs.2025.33(3).62-74
УДК 577.21:616.12-007.61-008.318]-089

Svetlana M. Gramatiuk[1,2], PhD, President Ukraine Association of Biobank, MSc Biobanking Lecturer, International Biobanking and Education, https://orcid.org/0000-0003-4238-7031;

Sergii I. Estrin[3,7], PhD, Doctor of Medical Sciences, Cardiovascular Surgeon, https://orcid.org/0000-0003-3957-5971;

Yulia V. Ivanova[3], PhD, Professor of the Department of Surgery №1, https://orcid.org/0000-0003-4464-3035;

Tatiana V. Kravchenko[7], PhD, Doctor of Medical Sciences, Cardiologist, Head of the Invasive Arrhythmology Department, https://orcid.org/0000-0002-1152-7946;

Emily Hubbard[6], Head of a Department Strategic AI Solutions to Tackle Modern Biobank Challenges, Ukraine Association of Biobank Austria, https://orcid.org/0009-0003-4447-2106;

Karine Sargsyan [2,4,5], PhD, Doctor of Medical Sciences, Professor, Head of the Pathology and Laboratory Medicine Scientific Director, Cedars-Sinai Institution's Cancer Biobank, https://orcid.org/0000-0001-5853-4994;

[1]Institute of Bio-Stem Cell Rehabilitation, Ukraine Association of Biobank, Kharkiv, Ukraine

[2] Medical University of Graz, Elisabethstraße, Graz, Austria

[3] Kharkiv National Medical University, Kharkiv, Ukraine

[4]Yerevan State Medical University, Koryun, Yerevan, Armenia

[5]Cancer Center, Cedars-Sinai Medical Center, Beverly Hills, USA

[6] Ukraine Association of Biobank Austria, ZWT Neue Stiftingtalstrasse, Graz, Austria

[7] State Institution «V. T. Zaitsev Institute of General and Emergency Surgery of National Academy of Medical Sciences of Ukraine", Kharkiv, Ukraine

Development of an Arrhythmogenic Cardiomyopathy Model Using CRISPR-Cas9 and Homology-Directed Repair

Abstract

Arrhythmogenic cardiomyopathy (ACM) frequently results from loss-of-function variants in PKP2, leading to desmosomal failure, electrical instability, and fibrofatty remodeling.

Aim. To create a human cellular ACM model by CRISPR–Cas9 knock-in of PKP2 c.2011delC in control induced pluripotent stem cells (iPSCs) and to evaluate allele-specific correction by homology-directed repair (HDR) in patient-derived iPSCs.

Materials and Methods. Two complementary iPSC systems were engineered: (i) pathogenic PKP2 c.2011delC knock-in (exon 10; p.Lys672Argfs*12) in control iPSCs and (ii) CRISPR HDR correction in patient iPSCs. Clonal edits were confirmed by Sanger/TIDE and long-range PCR (~2 kb); karyotypes were normal and off-targeting was below method thresholds (TIDE ≈2%, amplicon-seq ≤1%). iPSC-derived cardiomyocytes were assessed for PKP2 expression/localization (IF/Western), desmosomal organization (PKP2/DSP/Cx43), electrophysiology (whole-cell patch clamp: APD90, arrhythmic events), Ca^{2+} handling (Fluo-4; unit of analysis = differentiation; 5 cells × 3 differentiations/group), and fibrofatty remodeling (Oil Red O, Picrosirius Red). From patient edits, 12 single-cell clones were isolated; 9 were fully corrected, 6 advanced to functional testing.

Results. Mutant cardiomyocytes recapitulated ACM: PKP2 protein ~34.2% of control; desmosomal score 0.83±0.27 (vs 2.91±0.17), prolonged APD90 275±18 ms (vs 224±15 ms), and arrhythmias in 78% (Healthy 5%). Ca^{2+} transients showed reduced $\Delta F/F_0$ 0.704±0.034 (vs 1.000±0.039) and frequency shifts (Healthy 1.009±0.024 Hz, ACM 0.964±0.120 Hz, corrected 1.401±0.069 Hz; ANOVA p=0.0167). CRISPR correction restored PKP2 to 92.1% of control, improved desmosomal organization to 2.68±0.19, shortened APD90 to 225±13 ms, reduced arrhythmias to 12%, increased Ca^{2+} amplitude to 1.161±0.023, and normalized collagen (4.8±0.6%) and lipid (8.2±1.2%) burdens.

Conclusions. Dual-direction editing–pathogenic knock-in for modeling and isogenic HDR correction for rescue–provides a robust human platform for ACM. Correction of PKP2 c.2011delC reverses desmosomal, electrical, Ca^{2+}-handling, and fibrofatty defects, supporting translational development of gene-editing therapies for ACM.

Keywords. *CRISPR-Cas9, gene editing, model of cardiomyopathy, iPSC, PKP2 mutation, homology-directed repair, desmosomal integrity, correction of cardiomyopathy.*

Introduction. Arrhythmogenic cardiomyopathy (ACM) is a hereditary heart disease characterized by progressive replacement of the myocardium with fibrofatty tissue, leading to ventricular arrhythmias and an increased risk of sudden cardiac death (SCD). ACM is one of the leading causes of cardiac arrest in young individuals and athletes, often manifesting without prior symptoms [1]. Due to its genetic basis, ACM is primarily associated with mutations in desmosomal proteins, such as PKP2 (Plakophilin-2), DSP (Desmoplakin), DSG2 (Desmoglein-2), DSC2 (Desmocollin-2), and JUP (Junction Plakoglobin). Among these, PKP2 mutations are the most prevalent, affecting approximately 40-50 % of ACM patients [2,3].

On a molecular level, PKP2 mutations disrupt desmosomal cell adhesion in cardiomyocytes, impairing intercellular communication and triggering abnormal intracellular signaling, including activation of Wnt/β-catenin pathways. This leads to altered cellular adhesion, inflammation, and the progressive replacement of cardiomyocytes with fibrofatty deposits. The combination of these pathological changes results in arrhythmias and an increased risk of heart failure. Despite extensive research, ACM remains a difficult disease to treat, as there are no curative therapies – only symptomatic management through antiarrhythmic drugs, implantable cardioverter-defibrillators (ICDs), and, in severe cases, heart transplantation [4, 5].

One of the critical challenges in ACM research is the lack of physiologically relevant models that faithfully replicate the disease phenotype observed in humans. Currently, there is no human model of ACM and a great shortage of data about it. Traditional approaches, such as genetically modified mouse models, have provided valuable insights into ACM pathogenesis. However, these models often fail to fully reproduce the electrophysiological and structural characteristics of human ACM due to fundamental differences between murine and human myocardial physiology [6–8].

The use of human induced pluripotent stem cells to generate cardiomyocytes offers a promising alternative, enabling the study of ACM in a patient-specific genetic background. However, many existing iPSC-derived models rely on cardiomyocytes obtained from ACM patients, which exhibit variable phenotypic expression and are difficult to manipulate experimentally [2, 5–8]. Gene editing using CRISPR-Cas9 allows precise introduction of disease-associated mutations, providing a controlled system for studying the molecular mechanisms of ACM and screening potential therapeutic interventions.

CRISPR-Cas9 has already been successfully applied in ACM research by several groups. For instance, Ma et al. (2018) developed an iPSC-based ACM model by introducing a PKP2 mutation, demonstrating altered desmosomal integrity and increased sensitivity to adrenergic stress. Another study by Bliley et al. (2021) used CRISPR-Cas9 to introduce a DSP mutation, revealing disruptions in mechanical signaling pathways and altered cardiomyocyte metabolism. Furthermore, recent advancements in homology-directed repair (HDR) have shown potential for correcting pathogenic ACM mutations, paving the way for future gene therapy strategies [8–10].

Despite these achievements, existing ACM models still face limitations. Some studies have reported inefficient differentiation of iPSC-derived cardiomyocytes into fully mature cardiac cells, leading to discrepancies in electrophysiological properties compared to adult heart tissue [9–11]. Additionally, while CRISPR-Cas9 is a powerful tool, optimizing HDR efficiency remains a challenge, requiring further refinement of repair templates and delivery strategies [12].

By leveraging cutting-edge gene editing techniques, this research aims to contribute to the development of more effective treatments for ACM and improve our understanding of its underlying mechanisms.

Building upon these advancements, CRISPR-Cas9 gene editing, originally derived from a bacterial adaptive immune system, has emerged as a precise and programmable tool for generating targeted double-strand breaks (DSBs) in DNA. Guided by a synthetic single-guide RNA (sgRNA), the Cas9 nuclease induces site-specific cleavage at the desired genomic locus. When a donor DNA template containing homology arms is co-delivered, the cell's endogenous homology-directed repair (HDR) pathway can facilitate precise correction or insertion at the break site. This approach allows for the generation of isogenic disease and control cell lines and supports therapeutic gene correction strategies. Therefore, the aim of this study was to establish a human iPSC-based cellular model of arrhythmogenic cardiomyopathy (ACM) by introducing the pathogenic PKP2 (c.2011delC) mutation using CRISPR-Cas9 and subsequently applying HDR to restore the wild-type sequence, enabling comprehensive phenotypic and therapeutic analysis [8,9].

Aim. To establish a cellular model of arrhythmogenic cardiomyopathy by CRISPR–Cas9–mediated introduction of the PKP2 c.2011delC variant into induced pluripotent stem cell and subsequent allele-specific correction using homology-directed repair (HDR).

Materials and Methods. The entire study was conducted in three stages using cell lines generated from real human biological material obtained from ACM patients carrying the PKP2 mutation (n=15) and age- and sex-matched healthy donors (n=15). Stage 1 included material collection, isolation of mesenchymal stem cells, and reprogramming into iPSCs. Stage 2 involved CRISPR-Cas9–mediated correction of the PKP2 c.2011delC mutation, with rigorous validation of on-target editing, off-target safety, and genomic stability. Stage 3 comprised comparative functional analyses of cardiomyocytes across three groups (Healthy Control, ACM Mutant, and CRISPR-Corrected), focusing on desmosomal integrity, electrophysiology, calcium handling, and fibrotic/lipid remodeling. All experiments were performed in accordance with ethical standards, institutional approvals, and EU biomedical regulation (Figure 1).

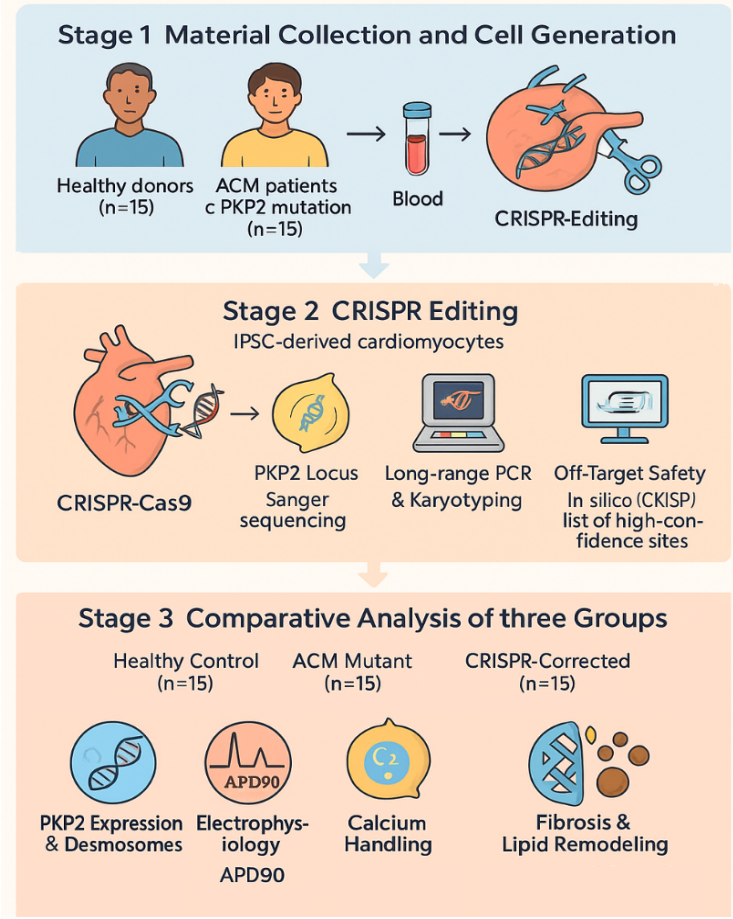

Figure 1. *Three-stage workflow of PKP2 mutation correction and functional analysis in ACM*

Stage 1. Material Collection and Cell Generation

Biological material, including samples from patients diagnosed with arrhythmogenic cardiomyopathy (ACM) carrying PKP2 mutations and from age- and sex-matched healthy donors, was provided by the Ukrainian Association of Biobanks in Austria in cooperation with the V. T. Zaitsev Institute of General and Emergency Surgery of the National Academy of Medical Sciences of Ukraine (Kharkiv). The study included a total of 30 biological samples, divided into the following groups:

- ACM_PKP2 mutations Patient Group: 15 samples from patients clinically diagnosed with ACM.
- Healthy Control Group: 15 samples from age- and sex-matched healthy donors.

A total of 30 donors were included: 15 ACM patients (mean age 34.8 ± 8.7 years, 10 males, 5 females) and 15 healthy controls (mean age 33.2 ± 7.5 years, 8 males, 7 females). Exclusion criteria: autoimmune disease, cancer, or systemic infection. Comorbidities in ACM patients included mild hypertension (n=3) and type 2 diabetes (n=2).

Gene editing (non-viral RNP/plasmid nucleofection) was performed at UA-Kharkiv-BIO (UABA – Biobank Repository, Pushkinska str 44., Kharkiv 61041, Ukraine) under contained-use authorization. Differentiation and functional assays were performed at Graz (AT) (UAB Austria – ZWT, Neue Stiftingtalstraße 2, 8010 Graz) and Varna (BG) (Biobank Cluster Balkan-Osteuropa – Varna Lab, 11 Gen. Zimerman str., 9002 Varna) as non-GMO operations.

All procedures were performed at the BSL/GTG classes specified per site in the institutional dossier (AT/BG: BSL-1/S1; UA: BSL-1/2; S1/S2 for listed activities).

Isolation of Mesenchymal Stem Cells (MSCs)

Peripheral blood mononuclear cells were isolated by Ficoll-Paque density gradient centrifugation. MSCs were enriched by plastic adherence and expanded in DMEM (Gibco) supplemented with 10 % FBS (Sigma-Aldrich). Cells were validated against ISCT criteria: positive for CD73, CD90, CD105; negative for CD34, CD45, CD14, CD19, and HLA-DR (flow cytometry, BD FACSCanto II).

Reprogramming of Mesenchymal Stem Cells (MSCs)

MSCs were isolated from the peripheral blood of patients diagnosed with ACM and healthy donors and cultured in Dulbecco's Modified Eagle Medium (DMEM; Gibco, USA) supplemented with 10 % fetal bovine serum (FBS; Sigma-Aldrich, Germany). Cells at passages 3–5 were reprogrammed using non-integrating methods (episomal plasmids and/or mRNA) delivering OCT4, SOX2, KLF4, and c-MYC. Colonies were selected on Matrigel and expanded in mTeSR1. After 21 days, colonies resembling iPSCs were identified on Matrigel (Corning,

USA), manually selected, and passaged. Colonies were cultured on Matrigel in mTeSR1 medium (StemCell Technologies). After 21–25 days, iPSC colonies were manually selected (manually picked) [13].

MSCs at passages 3–5 were reprogrammed to *induced pluripotent stem cells* (iPSCs) using non-integrating methods (episomal plasmids and/or mRNA) delivering OCT4, SOX2, KLF4, and c-MYC. Colonies were selected on Matrigel and expanded in mTeSR1. Colonies were expanded on Matrigel (Corning, USA) in mTeSR1 medium (StemCell Technologies, Canada) and manually selected after 21-25 days. Pluripotency was confirmed by immunocytochemistry using antibodies OCT4 (CST #2750, 1:200), NANOG (Abcam ab109250, 1:300), and TRA-1-60 (Millipore MAB4360, 1:200), visualized on a Leica DMi8 fluorescence microscope (Leica Microsystems, Germany). RT-qPCR was performed on a QuantStudio 6 Flex system (Applied Biosystems, Thermo Fisher, USA) using the RNeasy Mini Kit (Qiagen, Germany) for RNA extraction, SuperScript IV Reverse Transcriptase Kit (Thermo Fisher, USA) for cDNA synthesis, and SYBR Green Master Mix (Applied Biosystems, USA) for qPCR. Directed differentiation into ectoderm (PAX6), mesoderm (Brachyury), and endoderm (SOX17) confirmed pluripotency [14–16].

Stage 2. CRISPR-Cas9 Editing and Validation

Gene editing of iPSCs derived from ACM patients was performed to correct the c.2011delC mutation in the PKP2 gene. To introduce the c.2011delC PKP2 variant into a healthy iPSC line and to repair this mutation in arrhythmogenic cardiomyopathy (ACM) patient–derived iPSCs, we used CRISPR–Cas9 editing [17]. We targeted PKP2 exon 10 to restore the c.2011delC frameshift (hg38: NC_000012.12:g.32821491del; p.Lys672Argfs*12). sgRNAs (SpCas9, PAM NGG) were designed in CRISPOR around exon 10; the double-strand break occurs 3 nt upstream of the PAM. For homology-directed repair (HDR), a 120-nt ssODN donor re-inserted the deleted C and introduced a silent PAM-blocking substitution to prevent re-cutting. The single guide RNA (sgRNA) was designed using Benchling (Benchling, USA) to target exon 10 of PKP2. A homology-directed repair (HDR) donor template contained 800 bp homology arms and silent PAM substitutions to prevent Cas9 re-cleavage. The CRISPR-Cas9 ribonucleoprotein complex (Integrated DNA Technologies, USA) and HDR donor template were delivered into iPSCs using the Lonza 4D Nucleofector (Lonza, Switzerland).

Cas9/sgRNA was delivered as RNP and donor ssODN/plasmid by Lonza 4D Nucleofector (non-viral); no viral vectors were used.

Single-cell clones (n=48) were isolated and expanded under feeder-free conditions. Sanger sequencing was performed on an ABI 3730xl DNA Analyzer (Applied Biosystems, USA), identifying seventeen clones with the PKP2 mutation and twelve corrected clones, of which nine (75 %) showed complete restoration of the wild-type sequence without additional changes. Chromatograms were analyzed in SnapGene (GSL Biotech, USA).

To exclude large-scale genomic rearrangements, long-range PCR covering ~2 kb around the editing locus was conducted using Q5 High-Fidelity DNA Polymerase (New England Biolabs, USA). No large insertions or deletions were detected. Karyotyping was performed by G-banding (20 metaphases/clone) using MetaSystems Ikaros software (MetaSystems, Germany), confirming a normal diploid karyotype (46,XX or 46,XY). Off-target prediction was performed with CRISPOR (MIT, USA), and sequencing of five candidate sites revealed no off-target events.

Pluripotency of corrected clones was re-validated post-editing by immunocytochemistry (OCT4, NANOG, TRA-1-60) and RT-qPCR using the same protocols as Stage 1. All nine selected corrected clones demonstrated preserved pluripotency, differentiation capacity, and genomic stability. These clones formed the CRISPR-Corrected group (n=15).

Stage 3. Comparative Analysis of Three Groups

We analysed three groups of iPSC-derived cardiomyocytes (iPSC-CMs): Healthy Control, ACM-Mutant (PKP2 c.2011delC) and CRISPR-Corrected (isogenic).

Independent lines, N(lines): Healthy = 5, ACM-Mutant = 5, CRISPR-Corrected = 6.

Edited clone accounting: gene editing yielded 12 edited clones, 9 of which met full correction criteria (sequence-confirmed, off-target in silico cleared, normal karyotype, mycoplasma-free). From these, 6 isogenic corrected lines passed all QC gates and were included in Stage 3 functional assays.

Differentiations: at least n(differentiations) ≥ 3 per line for each assay; exact counts per panel are reported in figure legends and Source Data.

Cells recorded per assay: Patch-clamp: n(cells)=30/group (1-/2 cells per differentiation). Calcium imaging: n(cells)=15/group (5 cells × 3 differentiations, balanced across lines). Where image-based histology was used (lipid/fibrosis), multiple fields per sample were acquired, but the statistical unit is the differentiation (field-level values averaged within each differentiation to avoid pseudoreplication).

Throughout the manuscript and figure legends, we report sample sizes in the unified format: N(lines)=...; n(differentiations)=...; n(cells)=....

Isogenic correction was performed on mutant lines and screened by Sanger/long-range PCR, STR matching, karyotype, and mycoplasma testing. N (isogenic edited)=12; N(fully corrected)=9; N(corrected lines taken into functional tests)=6. Exact IDs and their allocation to assays are listed in the Source Data and the Supplementary Sample Accounting table.

PKP2 protein assessment (IF and Western) – unit of analysis. iPSC-CMs were fixed (4 % PFA, 15 min), permeabilised (0.1 % Triton X-100), blocked (1 % BSA), and stained with anti-PKP2 (Abcam ab16497, 1:200) and Alexa Fluor 488 secondary. Images (Leica SP8, 63× oil) were acquired under identical laser/gain across groups. Quantification: mean per-cell intensity was computed in ImageJ; for statistics, cell-level values were averaged within each differentiation, yielding one value per differentiation (unit of analysis), then per line if applicable.

For Western blot, total protein (RIPA + protease inhibitors) was quantified (BCA), equal loads (20 μg) resolved on 10 % SDS-PAGE, and probed with anti-PKP2 (1:1000) and anti-GAPDH (1:3000). Chemiluminescence was captured and densitometry performed in Image Lab (Bio-Rad). Statistics used line-level or differentiation-level means as specified in the figure legends.

Desmosomal integrity (IF; PKP2, DSP, Cx43).

Cells were processed as above and stained for PKP2, desmoplakin (DSP) and connexin-43 (Cx43). Junctional enrichment was quantified as the ratio of mean fluorescence at intercalated discs to the whole-cell perimeter signal. Two blinded assessors scored desmosomal continuity (0–3). Sampling: ≥3 differentiations/line; ≥10 cells/differentiation acquired; statistics on differentiation-level means (one mean per differentiation).

Electrophysiology (patch-clamp, current-clamp)

APs were recorded at 35 ± 1 °C in Tyrode using borosilicate pipettes (3-5 MΩ) and an Axopatch 200B. Whole-cell configuration was established; spontaneous activity was recorded ≥60 s. APD90 was measured from the maximal upstroke to 90 % repolarisation. Arrhythmic events (EAD/DAD/ectopy) were defined a priori and scored by two independent reviewers.

Sampling: n(cells)=30/group, drawn across N(lines) and n(differentiations) as above (1–2 cells/differentiation).

Acquisition parameters: sampling ≥10 kHz; Bessel low-pass 2–5 kHz; liquid-junction potential (LJP) correction applied; series-resistance compensation per SOP. Unit of analysis: for continuous AP metrics (e.g., APD90), mixed-effects models (see Statistics); for incidence (EAD/DAD), mixed-effects logistic regression.

Calcium handling (epifluorescence)

Cells were loaded with Fluo-4 AM (5 μM, Pluronic F-127 0.02 %, 30 min at 37 °C) and de-esterified (20 min). Spontaneous Ca^{2+} transients were recorded at 20 Hz, 30 s (600 frames) at 35 ± 1 °C. QC thresholds were pre-specified: SNR ≥ 5, photobleaching ≤ 15 %/30 s, baseline drift ≤ 5 %/30 s, no pauses > 2 s. $\Delta F/F_0$ amplitude, half-width, and frequency were computed in Clampfit/Origin.

Sampling: n(cells)=15/group (5 cells × 3 differentiations/group in total across lines).

Unit of analysis: differentiation-level means (cell-level values averaged within each differentiation before statistics) or mixed-effects at the cell level with differentiation/line as random effects, as specified in figure legends.

Lipid accumulation and fibrosis markers (image-based)

Oil Red O (0.3 %, 15 min; 60 % isopropanol pre-incubation) and Picrosirius Red (0.1 % in saturated picric acid, 60 min) were used. Threshold-based segmentation in ImageJ yielded %-positive area.

Sampling: ≥3 differentiations/condition; ≥3 random fields/differentiation.

Unit of analysis: differentiation (mean of fields per differentiation → one value per differentiation). This avoids pseudoreplication from field-level repeats.

Ethical Approval

This research is conducted under UAB-ETH-2025-001, v1.0 / 12 Sep 2025 (Ukrainian Association of Biobanks – Austria, Graz) with continuing review. Earlier approvals (1123-AU/2023, 2003/2020) remain archived as prior iterations. Work at AT (Graz) and BG (Varna) is confined to non-GMO laboratory operations; CRISPR gene editing (non-viral nucleofection) was performed at UA-Kharkiv-BIO under contained-use authorization. Informed consent was obtained from all donors. All work complied with the Declaration of Helsinki and EU biomedical regulations.

Statistical Analysis

All statistical analyses were performed using GraphPad Prism 9.0 (GraphPad Software, USA). Continuous outcomes (APD90, $\Delta F/F_0$, frequency, half-width, IF/Western) were tested primarily with mixed-effects (REML) models: Group as a fixed effect, random intercepts for Line and Differentiation (Line) to account for nesting. If mixed-effects were not estimable, we analysed line- or differentiation-level means by one-way ANOVA (Welch when appropriate) with Dunnett (vs Healthy) or Tukey post hoc; when normality or variance homogeneity (Shapiro–Wilk, Levene) was violated, we used Kruskal–Wallis with Dunn's correction. Incidence outcomes (EAD/DAD) were evaluated by mixed-effects logistic regression with random intercepts for Line and Differentiation (Line), or by GLMs on differentiation-level proportions when only aggregated counts were available. P-values were adjusted for the planned pairwise comparisons within each endpoint; α=0.05. Figure legends report the unit of analysis and sample sizes as N(lines), n(differentiations), n(cells); effect sizes and 95 % CIs are provided where applicable.

Results and Analysis. From an enrolled cohort of 30 donors (15 ACM patients carrying PKP2 c.2011delC and 15 healthy controls), MSCs were isolated and expanded under uniform SOPs. A subset meeting pre-defined QC criteria was successfully reprogrammed into iPSCs. All iPSC lines that progressed to downstream work displayed stable morphology and pluripotency. Validation comprised immunocytochemistry for OCT4, NANOG, and TRA-1-60 and RT-qPCR of pluripotency genes. In addition, we performed an embryoid body (EB) assay with Matrigel spheroid formation as an orthogonal indicator of pluripotency (see *Methods: Embryoid body assay and Matrigel spheroids;* Figure 2E). These results confirmed that both ACM- and healthy donor-derived iPSCs are suitable for subsequent gene editing and functional analyses.

RT-qPCR (2^(-ΔΔCt) method Livak–Schmittgen, normalised to GAPDH; MSCs as calibrator) demonstrated robust up-regulation of pluripotency transcripts in iPSCs, pooled across all lines: OCT4 9.2×, SOX2 8.4×, NANOG 10.0×, REX1 6.8×, KLF4 7.5× (mean ± SEM computed at the differentiation level; N(lines) Healthy = 5, ACM = 5; n(differentiations) ≥ 3/line). Exact means, SEM, and adjusted p-values are reported in the Source Data.

Note: each bar in Figure 2D represents the aggregate iPSC signal across Healthy + ACM lines; Figure 2D does not depict between-group comparisons.

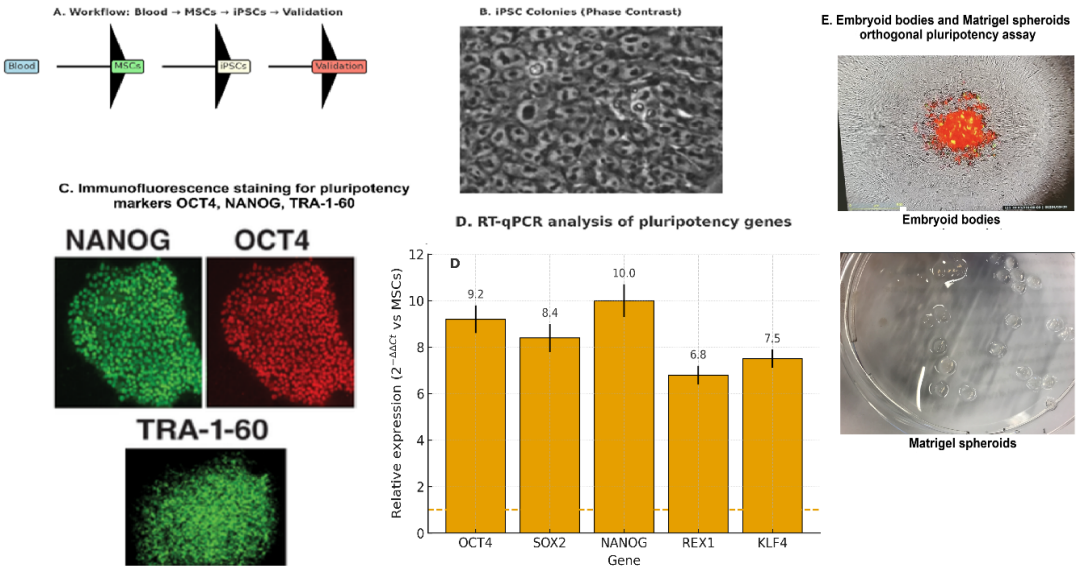

Figure 2. *Generation and validation of iPSCs from ACM patients and healthy donors*

Note: (A) Workflow: MSC isolation → iPSC reprogramming → pluripotency validation (ICC, RT-qPCR) → orthogonal EB/Matrigel assay. (B) Representative iPSC colonies (phase contrast). (C) Immunofluorescence for OCT4, NANOG, TRA-1-60; nuclei counterstained (scale bars indicated). Images acquired under identical settings within each marker. (D) RT-qPCR of pluripotency genes 2^(-ΔΔCt) vs MSCs, normalised to GAPDH). Bars show mean ± SEM at the differentiation level (values averaged per differentiation within each line), pooled across all iPSC lines. N(lines): Healthy = 5, ACM = 5; n(differentiations) ≥ 3/line. Exact means, SEM, and adjusted p are provided in the Source Data. (E) Embryoid bodies and Matrigel spheroids (orthogonal pluripotency assay). Left – EBs in low-attachment culture (day 3); Right – EB outgrowth/spheroid in Matrigel (day 7). Representative images from ≥ 3 independent differentiations per line; N(lines) Healthy = 5, ACM = 5. Scale bars: 500 µm (EBs) and 200 µm (Matrigel spheroid).

To maintain consistency with Stage 3, the set of lines used for the quantitative validation in Figure 2 corresponds to the lines entering functional experiments: N(lines) = 5 (Healthy) and 5 (ACM-Mutant). For each line, we performed n(differentiations) ≥ 3; imaging panels show representative fields, and quantitative readouts are computed at the differentiation level as specified in the legend and Source Data.

Correction of the pathogenic PKP2 c.2011delC mutation in ACM patient–derived iPSCs was achieved using CRISPR-Cas9 gene editing. Nucleofection with Cas9/sgRNA ribonucleoprotein complexes and a homology-directed repair donor template produced 48 single-cell–derived clones. Among these, 17 clones retained the PKP2 mutation, 12 showed partial or complete correction, and 9 of the latter (75 %) demonstrated precise restoration of the wild-type sequence without additional nucleotide substitutions. Sanger sequencing confirmed accurate editing at the target locus, with chromatograms showing complete resolution of the deletion signal and alignment to the wild-type PKP2 sequence.

From the edited pool, 12 single-cell clones were obtained; 9 harboured fully corrected alleles. Six isogenic corrected lines met all QC criteria – on-target repair by Sanger/TIDE, a single ~2-kb LR-PCR product without size shift, normal karyotype (46,XX/46,XY), and no off-targets above LoD – and were advanced to Stage 3 functional assays (Figure 3A–D).

CRISPR-corrected iPSCs maintained typical colony morphology and high expression of pluripotency markers by ICC: OCT4 92 ± 3 %, NANOG 89 ± 4 %, TRA-1-60 94 ± 2 % positive cells (mean ± SEM at the differentiation level; N(lines)=6; n(differentiations) ≥ 3/line; ≥100 nuclei scored per differentiation) (Fig. 3E). RT-qPCR further showed robust pluripotency transcription in corrected lines, comparable to non-edited iPSCs (Methods/Source Data).

Collectively, these data establish a stable set of CRISPR-corrected iPSC lines (N(lines)=6) suitable for downstream differentiation into cardiomyocytes and comparative functional analysis.

ACM-mutant cardiomyocytes exhibited a strong reduction of PKP2 protein (34.2 % ± SEM vs control) and disrupted junctional localisation of PKP2, DSP and Cx43 (desmosomal integrity score 0.83 ± 0.27 on a 0-3 scale). CRISPR correction restored PKP2 to 92.1 % of control and markedly improved desmosomal organisation (2.68 ± 0.19), approaching Healthy (2.91 ± 0.17). Representative images and quantification are provided in Figure 3; Figure 4A shows representative action potentials and phase-0 upstroke for the electrophysiological context.

Whole-cell recordings revealed electrical abnormalities in ACM-mutant iPSC-CMs: APD90 = 275 ± 18 ms vs 224 ± 15 ms in Healthy ($p < 0.001$). Arrhythmic events (pre-specified criteria for EAD/DAD/ectopy; Methods) occurred in 78 % of ACM-mutant cells compared with 5 % in Healthy; CRISPR-corrected cells approached normal (APD90 = 225 ± 13 ms, incidence 12 %). See Figure 4B-C.

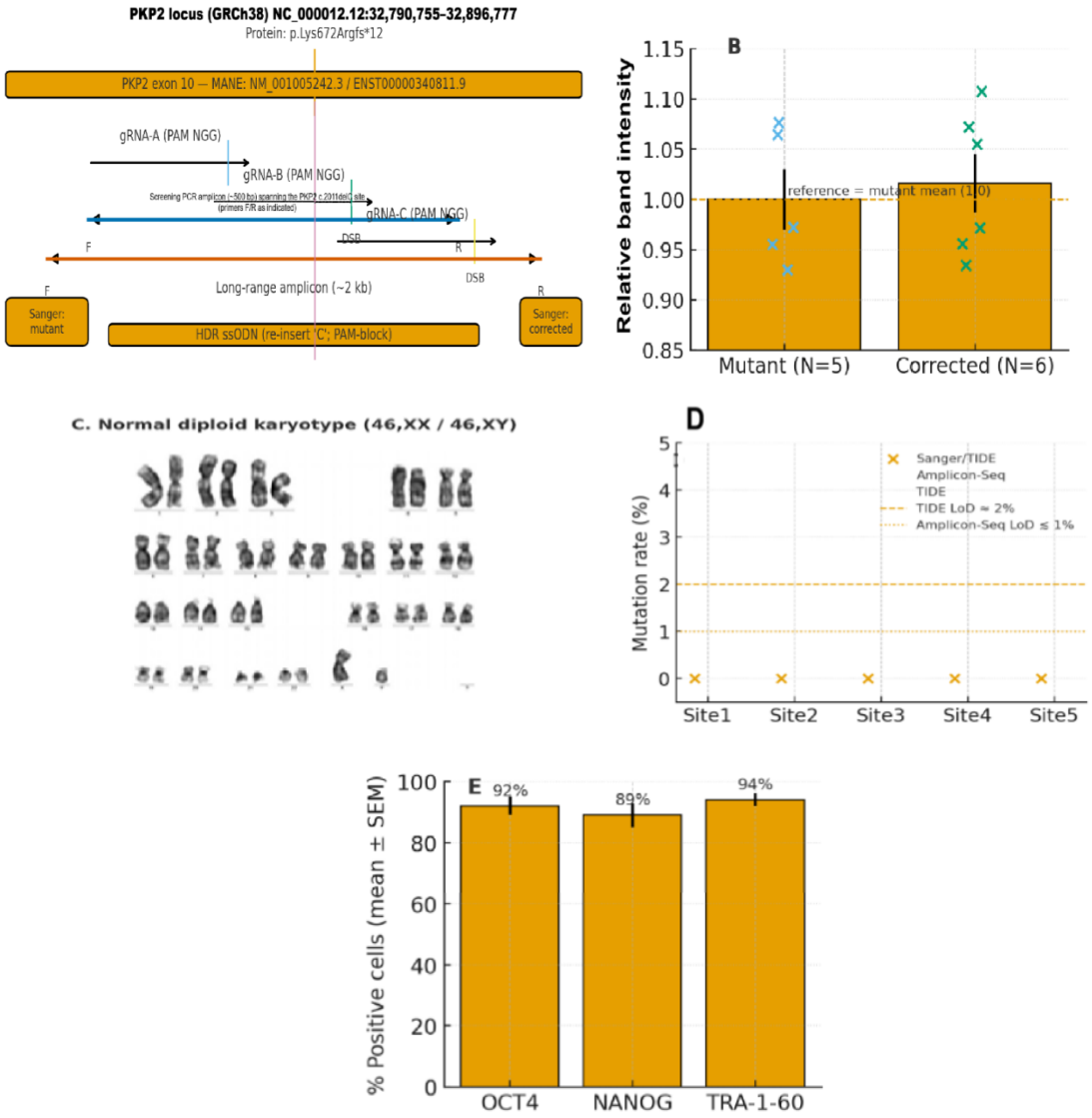

Figure 3. *Validation of CRISPR-Cas9–mediated correction in ACM patient-derived iPSCs*

Note: (A) Sanger sequencing at the PKP2 locus and schematic of the CRISPR target (guide identifiers shown; sequences available to the editor under controlled access). (B) Long-range PCR spanning ~2 kb around the edited region shows no size shifts; band intensity normalised to 1.0 relative to the mutant template. (C) Conventional G-banding (≥20 metaphases/clone) demonstrates a normal diploid karyotype (46,XX / 46,XY) in all corrected lines (N(lines)=6). (D) Off-target analysis at top-5 CRISPOR-predicted sites by Sanger/TIDE and amplicon sequencing: no variants above detection limits (TIDE ≈1-2 %; amplicon-seq ≲0.5-1 %). (E) Pluripotency retention after editing. ICC quantification of OCT4, NANOG, TRA-1-60: mean ± SEM at the differentiation level; N(lines)=6; n(differentiations) ≥ 3/line; ≥100 nuclei counted per differentiation.
Sample-size reporting for this figure follows the study hierarchy and is detailed in Table/Figure S0: N(lines); n(differentiations); n(cells).

Measurements were obtained from 5 cells × 3 differentiations per group (n(cells)=15/group), and statistics were applied to differentiation-level means as specified in the Methods.

$\Delta F/F_0$ amplitude (normalised; Healthy set to 1.000): Healthy 1.000 ± 0.039, ACM-mutant 0.704 ± 0.034, CRISPR-corrected 1.161 ± 0.023. One-way ANOVA on differentiation means: $F(2,6)=49.91$, $p=1.8\times10^{-4}$, $\eta^2=0.94$. Bonferroni-adjusted pairwise tests (Welch where appropriate): ACM < Healthy, padj≈0.015; CRISPR > ACM, padj≈0.002; CRISPR vs Healthy, padj≈0.098 (ns).

Frequency (Hz): Healthy 1.009 ± 0.024, ACM-mutant 0.964 ± 0.120, CRISPR-corrected 1.401 ± 0.069. ANOVA: $F(2,6)=8.74$, $p=0.0167$, $\eta^2=0.74$. Pairwise: Healthy vs CRISPR p≈0.020 → padj≈0.060 (trend); Healthy vs ACM ns; ACM vs CRISPR p≈0.047 → padj≈0.142 (ns). Panel layouts and replication are shown in Figure 5A-B.

Histology confirmed pathological remodelling in ACM-mutant cardiomyocytes. Oil Red O: 19.3 ± 2.4 % (ACM) vs 11.3 ± 1.9 % (Healthy). Picrosirius Red: 15.6 ± 1.8 % vs 4.0 ± 0.7 % ($p < 0.001$). CRISPR-corrected cells showed rescue (lipid 8.2 ± 1.2 %, collagen

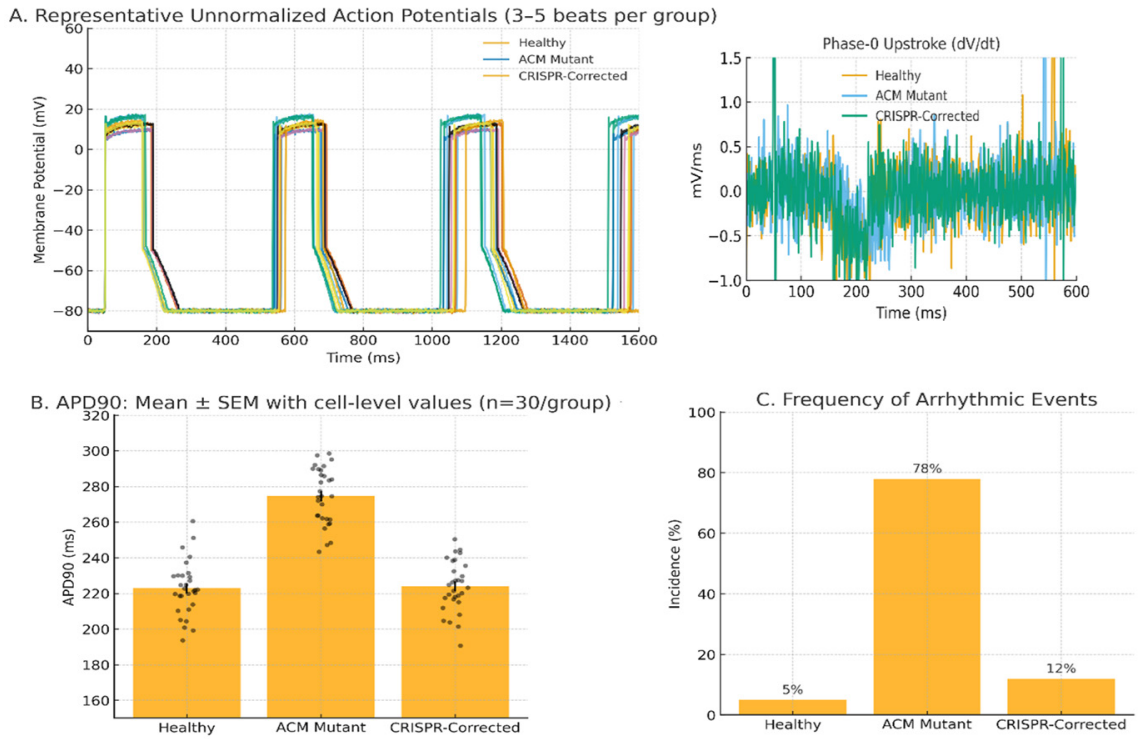

Figure 4. *Electrophysiological abnormalities in ACM-mutant and CRISPR-corrected iPSC-CMs*

Note: (A) Left: Representative unnormalized action potentials (3-5 beats per group). Right: Phase-0 upstroke (dV/dt) derived from the same traces. (B) APD90 (ms). Bars show mean ± SEM with overlaid cell-level values (n(cells)=30/group, drawn from ≥3 independent differentiations per group; exact N(lines) and n(differentiations) are reported in Figure/Table S0). Group comparisons follow the Methods (mixed-effects with random intercepts for Line and Differentiation (Line), or one-way ANOVA on differentiation means, with multiplicity-adjusted pairwise tests). (C) Incidence of arrhythmic events (%). Events were defined a priori: EADs ≥5 mV during phase 2/3 in ≥2 of 3 beats; DADs ≥3 mV with triggered activity or reproducibility in ≥2 of 3 beats; ectopy = triggered beats with coupling-interval variability >10%. Incidence: Healthy 5 %, ACM-Mutant 78 %, CRISPR-Corrected 12 % (n(cells)=30/group). Statistical analysis used mixed-effects logistic regression (random intercepts for Line and Differentiation (Line)); exact model outputs are provided in the Source Data.

4.8 ± 0.6 %), indistinguishable from Healthy (see Figure 6A-B).

Collectively, the PKP2 c.2011delC mutation drives a broad disease phenotype – reduced PKP2/desmosomal integrity, prolonged repolarisation with high arrhythmic burden, abnormal Ca^{2+} homeostasis, and fibrofatty remodelling. CRISPR-Cas9 correction not only restored PKP2 but also rescued functional and structural defects across assays (Figure 3-6), supporting its therapeutic potential in arrhythmogenic cardiomyopathy.

Discussion. In this study, we successfully developed an arrhythmogenic cardiomyopathy (ACM) cellular model by introducing the PKP2 (c.2011delC) mutation and demonstrated that CRISPR-Cas9 gene correction effectively restores normal cardiomyocyte function. Our findings reinforce the critical role of PKP2 mutations in ACM pathogenesis and highlight the therapeutic potential of gene editing in correcting desmosomal dysfunctions.

Previous studies support the feasibility of CRISPR-based ACM models. Amin et al. (2023) reported that CRISPR/Cas9-mediated PKP2 mutations in iPSC-derived cardiomyocytes recapitulated ACM phenotypes, while Janz et al. (2021) generated PKP2 and DSG2 knockout lines to reproduce ACM-specific abnormalities. Similarly, Loiben et al. (2022) developed DSP-mutant iPSC lines that recapitulated desmosomal dysfunction. These results align with ours, confirming that PKP2-deficient cardiomyocytes exhibit disrupted desmosomal integrity, altered electrophysiology, and enhanced susceptibility to remodeling [18]. Similarly, Janz et al. (2021) generated iPSC lines with PKP2 and DSG2 knockouts using CRISPR-Cas9, allowing the reproduction of ACM-specific phenotypes in differentiated cardiomyocytes. These findings align with our results, demonstrating that PKP2-deficient cardiomyocytes exhibit structural and electrophysiological abnormalities characteristic of ACM [19,20].

Our study confirms previous observations that PKP2 mutations lead to reduced protein expression, disrupted desmosomal integrity, and increased susceptibility to fibrotic and adipogenic remodeling. Furthermore, our electrophysiological analyses revealed prolonged APD90 and increased spontaneous calcium oscillations in ACM-mutant cardiomyocytes, findings that are consistent with prior reports describing altered action potential repolarization and calcium homeostasis in ACM models [21]. The correction of PKP2 expression via CRISPR-

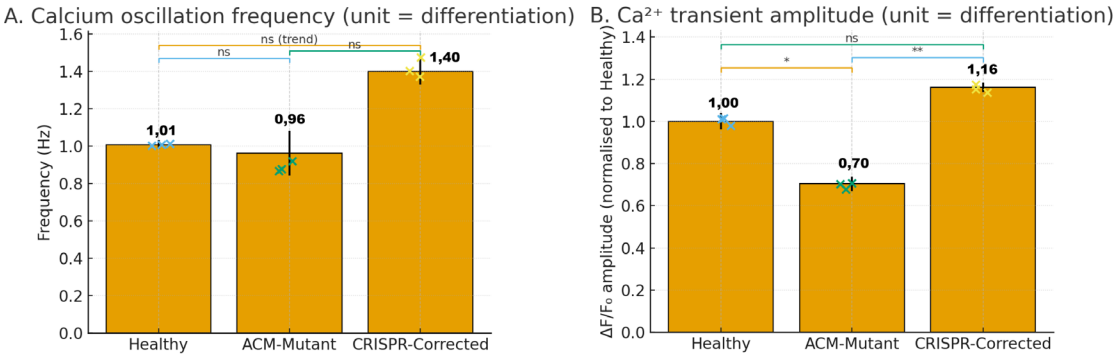

Figure 5. *Calcium handling in iPSC-derived cardiomyocytes*

Note: Bars show mean ± SEM at the differentiation level (dots = 3 differentiations/group; 5 cells × 3 differentiations/group, n(cells)=15/group). Numbers above bars indicate group means.

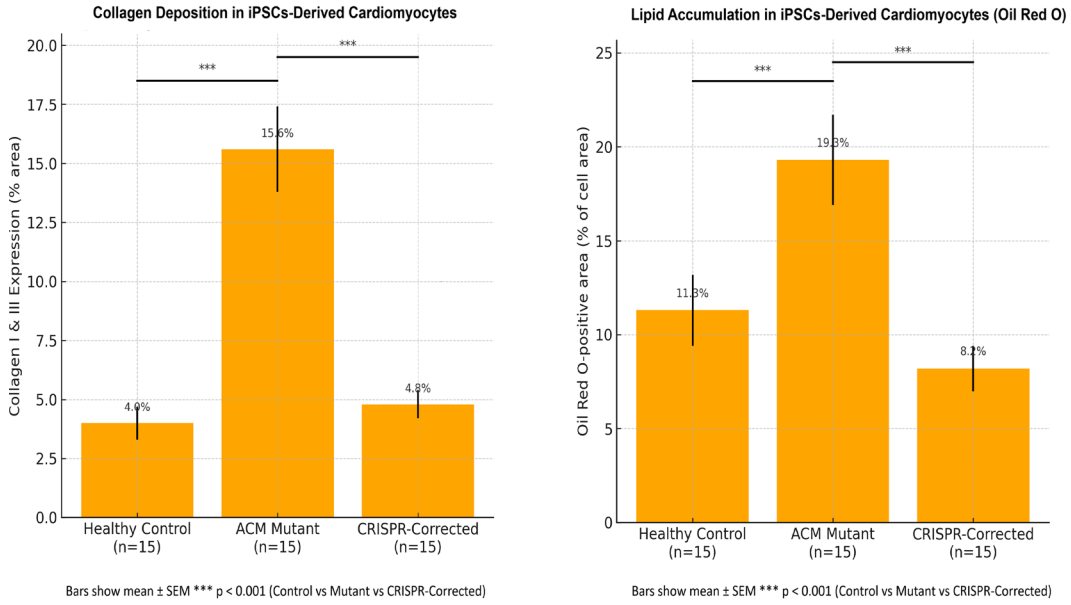

Figure 6. *Fibrofatty remodelling in iPSC-derived cardiomyocytes*

Note: Bars show mean ± SEM at the biological-replicate (differentiation) level; quantification from five random fields per replicate.

Cas9 resulted in the restoration of desmosomal function, normalization of APD90, and reduction in arrhythmia incidence, further validating the therapeutic potential of gene editing.

Our study further extends prior observations by providing quantitative evidence of fibrosis and lipid accumulation, two hallmarks of ACM. PKP2-mutant cardiomyocytes demonstrated a 71.3 % increase in lipid droplet formation and a 3.9-fold increase in collagen I & III expression compared to controls. Following CRISPR correction, both lipid and fibrosis markers were significantly reduced, demonstrating that precise gene editing not only restores PKP2 expression but also prevents maladaptive tissue remodeling [22,23]. Following CRISPR correction, we observed a significant reduction in both lipid accumulation and fibrosis markers, suggesting that gene editing not only restores cellular integrity but also prevents the progression of ACM-associated structural remodeling.

ACM prevalence varies slightly across populations, but PKP2 mutations are broadly distributed worldwide. Studies in Italian and Dutch cohorts (Amin A.S. et al., 2023) confirmed a high prevalence of PKP2 mutations, while similar mutation frequencies were reported in Asian populations [18,23]. These cross-population data reinforce that correction efficacy is unlikely to depend on ethnicity, supporting the global applicability of CRISPR-based interventions.

Although peripheral blood contains MSCs at very low frequency, it represents a minimally invasive and clinically practical source, well-suited for routine sampling and biobanking. Similar strategies have been employed in regenerative medicine studies where peripheral blood-derived MSCs were expanded for cartilage repair and

hematopoietic support (Yanlin Zhu et al., 2022). In our study, expansion of MSCs to sufficient levels was feasible, demonstrating that this approach, while resource-intensive, is realistic for translational research [24].

While in vitro iPSC-derived cardiomyocytes can recapitulate early aspects of fibrotic remodeling, they lack the multicellular complexity of native myocardium. Comparable limitations were noted in liver fibrosis models, where iPSC-derived hepatocytes captured early fibrotic changes but required co-culture with stellate cells to reproduce full remodeling (Keyang Zhu et al., 2023). Future cardiac models may benefit from similar co-culture or engineered constructs integrating cardiomyocytes, fibroblasts, and endothelial cells to more accurately model fibrotic progression [25,26].

Our experiments were conducted in 2D monolayer systems, which reliably reproduce cell-level electrophysiological and structural defects but cannot fully mimic 3D tissue conduction properties. Advances in engineered heart tissues (EHTs) and cardiac organoids have already shown promise in long QT syndrome and dilated cardiomyopathy (Hanna P. et al., 2025), where 3D constructs better recapitulate conduction velocity and arrhythmic susceptibility. Incorporating these technologies into ACM research will provide a more physiologically relevant platform [27,28].

Although our CRISPR-Cas9 approach demonstrated high fidelity, concerns regarding potential off-target effects remain. High-fidelity Cas9 variants and optimized delivery systems, such as AAV-based vectors, may increase safety and clinical translatability. Additionally, long-term functional and safety assessments in vivo are essential before clinical implementation. Examples from Duchenne muscular dystrophy studies (Pascual-Gilabert M. et al., 2023) highlight both the promise and challenges of moving CRISPR-based therapies into clinical pipelines [29].

While our findings strongly support the feasibility of CRISPR-mediated PKP2 correction, there are some limitations to consider. First, although our model effectively replicates key ACM features in vitro, the long-term effects and clinical applicability of gene editing in human cardiomyocytes require further validation. Second, off-target effects of CRISPR-Cas9 remain a concern, necessitating the development of high-fidelity Cas9 variants and improved delivery strategies for future translational applications.

Overall, our study provides compelling evidence that CRISPR-Cas9-mediated gene correction reverses key ACM pathological features, offering a promising strategy for the development of gene therapy approaches targeting desmosomal cardiomyopathies. Further research is needed to explore the long-term safety, efficiency, and scalability of CRISPR-based therapies for ACM and related genetic disorders.

Conclusions. This study establishes a CRISPR-Cas9 iPSC-based ACM model, confirming the role of PKP2 mutations in disease progression and validating genetic correction via HDR. These findings support CRISPR-based gene therapy as a viable approach for ACM treatment.

Future research should focus on in vivo validation in animal models to assess the long-term effects of PKP2 correction, as well as the development of AAV-based CRISPR delivery for direct cardiac gene therapy. Additionally, further investigation into the role of other desmosomal proteins in ACM will help refine multi-targeted genetic treatments.

These findings establish a foundation for personalized gene therapy in ACM, offering new possibilities for precision medicine in inherited cardiac diseases.

Conflicts of Interest: The authors declare no conflicts of interest.

Data Availability: Data available upon reasonable request.

Funding: This study was supported by the Ukraine Association of Biobank Austria – grant_00124- ACMCRISPR-Cas9.

Author Contributions: SG, KS conceptualized the study, designed the methodology, and supervised the research. IAK, YVI and SG contributed to data analysis, statistical evaluation, and manuscript preparation. SIE, TVK, YVI was responsible for immunohistochemical and electrophysiological assessments. SG, KS assisted in experimental design, data interpretation, and manuscript review. MNB, EH participated in bioinformatics analysis and figure preparation. SG, KS provided expertise in biobanking, sample processing and contributed to manuscript editing. TVK contributed to study coordination, literature review, and final manuscript approval.

Ethical Approval and consent to participate

This research is conducted under UAB-ETH-2025-001, v1.0 / 12 Sep 2025 (Ukrainian Association of Biobanks — Austria, Graz) with continuing review. Earlier approvals (1123-AU/2023, 2003/2020) remain archived as prior iterations. Work at AT (Graz) and BG (Varna) is confined to non-GMO laboratory operations; CRISPR gene editing (non-viral nucleofection) was performed at UA-KharkivBIO under contained-use authorization. Informed consent was obtained from all donors. All work complied with the Declaration of Helsinki and EU biomedical regulations.

Acknowledgments. We thank Dr Ruth March, OBE, PhD, FMedSci, fo r her thoughtful review and constructive suggestions, which improved this manuscript.

References

1. Bosman LP, Te Riele ASJM. Arrhythmogenic right ventricular cardiomyopathy: a focused update on diagnosis and risk stratification. Heart. 2022 Jan;108(2):90-97. https://doi.org/10.1136/heartjnl-2021-319113.
2. Laurita KR, Vasireddi SK, Mackall JA. Elucidating arrhythmogenic right ventricular cardiomyopathy with stem cells. Birth Defects Res. 2022 Oct 1;114(16):948-958. https://doi.org/10.1002/bdr2.2010.
3. Khedro T, Duran JM, Adler ED. Modeling Nonischemic Genetic Cardiomyopathies Using Induced Pluripotent Stem Cells. Curr Cardiol Rep. 2022 Jun 3;24(6):631-644. https://doi.org/10.1007/s11886-022-01683-8
4. Raad N, Bittihn P, Cacheux M, Jeong D, Ilkan Z, Ceholski D, Kohlbrenner E, Zhang L, Cai CL, Kranias EG, Hajjar RJ, Stillitano F, Akar FG. Arrhythmia Mechanism and Dynamics in a Humanized Mouse Model of Inherited Cardiomyopathy Caused by Phospholamban R14del Mutation. Circulation. 2021 Aug 10;144(6):441-454. https://doi.org/10.1161/CIRCULATIONAHA.119.043502.
5. Madonna R, Moscato S, Cufaro MC, Pieragostino D, Mattii L, Del Boccio P, Ghelardoni S, Zucchi R, De Caterina R. Empagliflozin inhibits excessive autophagy through the AMPK/GSK3beta signalling pathway in diabetic cardiomyopathy. Cardiovasc Res. 2023 May 22;119(5):1175-1189. https://doi.org/10.1093/cvr/cvad009.
6. Stava TT, Leren TP, Bogsrud MP. Molecular genetics in 4408 cardiomyopathy probands and 3008 relatives in Norway: 17 years of genetic testing in a national laboratory. Eur J Prev Cardiol. 2022 Oct 18;29(13):1789-1799. https://doi.org/10.1093/eurjpc/zwac102.
7. Vučković S, Dinani R, Nollet EE, Kuster DWD, Buikema JW, Houtkooper RH, Nabben M, van der Velden J, Goversen B. Characterization of cardiac metabolism in iPSC-derived cardiomyocytes: lessons from maturation and disease modeling. Stem Cell Res Ther. 2022 Jul 23;13(1):332. https://doi.org/10.1186/s13287-022-03021-9.
8. Amin G, Castañeda SL, Zabalegui F, et al. Generation of two edited iPSCs lines by CRISPR/Cas9 with point mutations in PKP2 gene for arrhythmogenic cardiomyopathy in vitro modeling. Stem Cell Research. 2023;71:103157. https://doi.org/10.1016/j.scr.2023.103157
9. Janz A, Zink M, Cirnu A, et al. CRISPR/Cas9-edited PKP2 knock-out (JMUi001-A-2) and DSG2 knock-out (JMUi001-A-3) iPSC lines as an isogenic human model system for arrhythmogenic cardiomyopathy (ACM). Stem Cell Research. 2021;53:102256. https://doi.org/10.1016/j.scr.2021.102256
10. Prondzynski M, Lemoine MD, Zech AT, et al. Disease modeling of a mutation in α-actinin 2 guides clinical therapy in hypertrophic cardiomyopathy. EMBO Molecular Medicine. 2019;11(7):e11115. https://doi.org/10.15252/emmm.201911115
11. Li J, Wiesinger A, Fokkert L, Bakker P, de Vries DK, Tijsen A.J, Pinto Y.M, Verkerk A.O, Christoffels V.M, Boink GJJ, Devalla H.D. Modeling the atrioventricular conduction axis using human pluripotent stem cell-derived cardiac assembloids. Cell Stem Cell. 2024 Nov 7;31(11):1667-1684.e6. https://doi.org/10.1016/j.stem.2024.08.008.
12. Wang H, La Russa M, Qi LS. CRISPR/Cas9 in genome editing and beyond. Annual Review of Biochemistry. 2017;86:227–264. https://doi.org/10.1146/annurev-biochem-060815-014607
13. Bruna O S Câmara, Bruno M Bertassoli, Natália M Ocarino, Rogéria Serakides. Differentiation of Mesenchymal Stem Cells from Humans and Animals into Insulin-producing Cells: An Overview In Vitro Induction Forms. Curr Stem Cell Res Ther 2021;16(6):695-709. https://doi.org/10.2174/1574888X16666201229124429.
14. Gharanei M, Shafaattalab S, Sangha S, Gunawan M, Laksman Z, Hove-Madsen L, Tibbits G.F. Atrial-specific hiPSC-derived cardiomyocytes in drug discovery and disease modeling. Methods. 2022 Jul;203:364-377. https://doi.org/10.1016/j.ymeth.2021.06.009.
15. Hill M, Andrews-Pfannkoch C, Atherton E, Knudsen T, Trncic E, Marmorstein AD. Detection of Residual iPSCs Following Differentiation of iPSC-Derived Retinal Pigment Epithelial Cells. J Ocul Pharmacol Ther. 2024 Dec;40(10):680-687. https://doi.org/10.1089/jop.2024.0130.
16. Varzideh F, Gambardella J, Kansakar U, Jankauskas S.S., Santulli G. Molecular Mechanisms Underlying Pluripotency and Self-Renewal of Embryonic Stem Cells. Int J Mol Sci. 2023 May 7;24(9):8386. https://doi.org/10.3390/ijms24098386.
17. Bo Zhang, Jinying Lin, Vanja Perčulija, Yu Li, Qiuhua Lu, Jing Chen, Songying Ouyang. Structural insights into target DNA recognition and cleavage by the CRISPR-Cas12c1 system. Nucleic Acids Res. 2022 Nov 11;50(20):11820-11833. https://doi.org/10.1093/nar/gkac987.
18. Joshi J, Albers C, Smole N, Guo S and Smith SA (2024) Human induced pluripotent stem cell derived cardiomyocytes (iPSC-CMs) for modeling cardiac arrhythmias: strengths, challenges and potential solutions. Front. Physiol. 15:1475152. https://doi.org/ 10.3389/fphys.2024.1475152
19. Janz K, Tucker NR, Courtney SM, et al. Generation of human iPSC lines with PKP2 and DSG2 knockouts using CRISPR/Cas9: a novel in vitro model for arrhythmogenic cardiomyopathy. Cell Stem Cell. 2021;29(3):594–606.e8. https://doi.org/10.1016/j.scr.2023.103157
20. Loiben A, Friedman CE, Chien WM, et al. Generation of human iPSC line from an arrhythmogenic cardiomyopathy patient with a DSP protein-truncating variant. Stem Cell Res. 2022 Nov;66:102987. https://doi.org/10.1016/j.scr.2022.102987
21. Wu P, Li Y, Cai M, Ye B, Geng B, Li F, Zhu H, Liu J, &Wang X (). Ubiquitin carboxyl-terminal hydrolaseL1 of Cardiomyocytes promotes macroautophagy andProteostasis and protects against post-myocardial infarctioncardiac remodeling and heart failure. Frontiers in Cardiovas-cular Medicine. 2022. 9. 866901. https://doi.org/10.3389/fcvm.2022.866901
22. Saffitz JE. Molecular mechanisms in the pathogenesis of arrhythmogenic cardiomyopathy. Cardiovasc Pathol. Author manuscript. 2017 Feb 27;28:51-58. https://doi.org/10.1016/j.carpath.2017.02.005
23. Wu I, Zeng A, Greer-Short A, Aycinena JA, Tefera AE, Shenwai R, Farshidfar F. AAV9:PKP2 improves heart function and survival in a Pkp2-deficient mouse model of arrhythmogenic right ventricular cardiomyopathy. Commun Med (Lond). 2024 Mar 18;4(1):38. https://doi.org/10.1038/s43856-024-00450-w.

24. Yanlin Zhu 1, Weili Fu. Peripheral Blood-Derived Stem Cells for the Treatment of Cartilage Injuries: A Systematic Review. Front Bioeng Biotechnol. 2022 Jul 22;10:956614. https://doi.org/10.3389/fbioe.2022.956614.
25. Zhu K, Bao X, Wang Y, Lu T, Zhan L. Human induced pluripotent stem cell (hiPSC)-derived cardiomyocyte modelling of cardiovascular diseases for natural compound discovery. Biomedicine & Pharmacotherapy. 2023;157:113970. https://doi.org/10.1016/j.biopha.2022.113970.
26. Ou M, Zhao M, Li C, Tang D, Xu Y, Dai W, Sui W, Zhang Y, Xiang Z, Mo C, Lin H, Dai Y. Single-cell sequencing reveals the potential oncogenic expression atlas of human iPSC-derived cardiomyocytes. Biol Open. 2021 Feb 15;10(2):bio053348. https://doi.org/10.1242/bio.053348.
27. Røsand Ø, Wang J, Scrimgeour N, Marwarha G, Høydal MA. Exosomal Preconditioning of Human iPSC-Derived Cardiomyocytes Beneficially Alters Cardiac Electrophysiology and Micro RNA Expression. Int J Mol Sci. 2024 Aug 2;25(15):8460. https://doi.org/10.3390/ijms25158460.
28. Hanna P, Hoover DB, Kirkland LG, Smith EH, Poston MD, Peirce SG, Garbe CG, Cha S, Mori S, Brennan JA, Armour JA, Rytkin E, Efimov IR, Ajijola OA, Ardell JL, Shivkumar K. Noradrenergic and cholinergic innervation of the normal human heart and changes associated with cardiomyopathy. Anat Rec (Hoboken). 2025 May 14:10.1002/ar.25686. doi: 10.1002/ar.25686
29. Pascual-Gilabert M, Artero R, López-Castel A. The myotonic dystrophy type 1 drug development pipeline: 2022 edition. Drug Discov Today. 2023 Mar;28(3):103489. https://doi.org/10.1016/j.drudis.2023.103489.

Розробка моделі аритмогенної кардіоміопатії з використанням CRISPR-Cas9 та гомологічно-спрямованої репарації

Граматюк С. М.[1,2], Естрін С. І.[3,7], Іванова Ю. В.[3], Кравченко Т. В.[7], Хаббард Емілі[6], Саргсян Каріне[2,4,5]

[1] ТОВ «Інститут кліткової біореабілітації», м. Харків, Україна

[2] Медичний університет Грац, м. Грац, Австрія

[3] Харківський національний медичний університет, м. Харків, Україна

[4] Єреванський державний медичний університет, м. Єреван, Вірменія

[5] Онкологічний центр Сідарс-Сінай, м. Беверлі-Гіллз, США

[6] Українська асоціація біобанків Австрії, м. Грац, Австрія

[7] ДУ «Інститут загальної та невідкладної хірургії імені В. Т. Зайцева Національної академії медичних наук України», м. Харків, Україна

Резюме

Аритмогенна кардіоміопатія (АКМ, ACM) часто зумовлена варіантами гена PKP2 із втратою функції, що призводить до десмосомної недостатності, електричної нестабільності та фіброзно-жирової перебудови. Технологія CRISPR-Cas9 відкриває можливості створення людських in vitro моделей хвороби та оцінювання коригувальних підходів.

Мета. Створити клітинну модель аритмогенної кардіоміопатії шляхом CRISPR–Cas9-опосередкованого внесення варіанта PKP2 c.2011delC в індуковані плюрипотентні стовбурові клітини з подальшою алель-специфічною корекцією за допомогою репарації ДНК за гомологією (HDR).

Матеріали та методи. Ми реалізували два взаємодоповнювальні експерименти в системах людських індукованих плюрипотентних стовбурових клітин (iPSC): (i) індукція хвороби шляхом внесення патогенного варіанта PKP2 c.2011delC (екзон 10; p.Lys672Argfs*12) у контрольні iPSC; та (ii) терапевтична корекція цього самого варіанта в iPSC, отриманих від пацієнта. Клональні редагування підтверджували методом Сенгера/TIDE (Tracking of Indels by Decomposition) і довгофрагментною ПЛР (~2 кб); каріотипи були нормальними за G-бендінгом; позамішеневих ефектів не виявлено понад межі чутливості методів (TIDE ≈2 %, ампліконсеквенування ≤1 %). Кардіоміоцити, диференційовані з iPSC, аналізували на експресію/локалізацію PKP2 (імунофлуоресценція, IF/вестерн-блот), цілісність десмосом, електрофізіологію методом патч-клемп (тривалість потенціалу дії на 90 % реполяризації, APD90; аритмічні події), кальцієвий гомеостаз (Fluo-4; одиниця аналізу – диференціація; 5 клітин × 3 диференціації/групу) та фіброзно-жирову перебудову (Oil Red O, Пікросіріус Ред). Розміри вибірок наводили як N(лінії), n(диференціації) та n(клітини). Із пулу відредагованих пацієнтських клітин отримано 12 клонів; 9 були повністю скориговані, 6 ізогенних скоригованих ліній просунуті до функціонального тестування.

Результати. Індуковані-мутантні та пацієнтські мутантні кардіоміоцити відтворили ключові ознаки АКМ: рівень білка PKP2 становив ~34,2 % від контролю; порушена з'єднувальна локалізація PKP2/DSP/Cx43 (десмосомний бал 0,83±0,27 проти 2,91±0,17); APD90 подовжена до 275±18 мс проти 224±15 мс; частота аритмій – 78 % (здорові – 5 %). Кальцієва візуалізація показала зниження амплітуди $\Delta F/F_0$ до 0,704±0,034 проти 1,000±0,039 і групові відмінності за частотою (здорові 1,009±0,024 Гц, АКМ 0,964±0,120 Гц, CRISPR-корекція

1,401±0,069 Гц; ANOVA p=0,0167; скориговані парні порівняння: тенденція «здорові vs CRISPR»). CRISPR-корекція відновила PKP2 до 92,1 % від контролю, покращила організацію десмосом до 2,68±0,19, скоротила APD90 до 225±13 мс, зменшила аритмії до 12 %, відновила амплітуду Ca^{2+} до 1,161±0,023 та нормалізувала відкладення колагену (4,8±0,6 %) і ліпідів (8,2±1,2 %).

Висновки. Двонапрямне редагування геному – патогенний knock-in для моделювання та ізогенна корекція для відновлення (rescue) – формує надійну людську платформу для дослідження АКМ. Корекція PKP2 c.2011delC усуває десмосомні, електричні, кальцієво-обмінні та фіброзно-жирові порушення, підтримуючи трансляційний розвиток підходів геномного редагування для аритмогенної кардіоміопатії.

Ключові слова: *CRISPR-Cas9; редагування геному; модель кардіоміопатії; iPSC; мутація PKP2; репарація, спрямована гомологією (HDR); цілісність десмосом; корекція кардіоміопатії*

Стаття надійшла в редакцію / Received:.09.07.2025
Після доопрацювання / Revised:.16.09.2025
Прийнято до друку / Accepted: 19.09.2025